
A robust SPH formulation for solids

Bertrand Maurel* — **Alain Combescure*** — **Serguei Potapov****

* *Laboratoire de Mécanique des contacts et des Solides
INSA de Lyon/UMR CNRS
20 avenue Albert Einstein F-69621 Villeurbanne cedex*

** *Electricité de France, Direction des Etudes et Recherches
1 avenue du général de Gaulle BP 408, F-92141 Clamart cedex*

ABSTRACT. The smoothed particle hydrodynamics method such as other meshless methods is a very efficient numerical method for some types of modelling such as fracturing of solids. This technique, initially developed for fluid or gas, was extended to solids but it suffers from severe instability problems. The origins of these instabilities have been identified by the SPH community and solutions were developed to remove them. An overview of the different proposed techniques is presented. Among them it appears that for solids the use of the total Lagrangian formulation is the most simple and valuable solution. In the same time stress points can be added to this new formulation in order to improve accuracy and convergence rate despite an increase in computational cost.

RÉSUMÉ. La méthode SPH (Smoothed Particle Hydrodynamics) comme les autres méthodes sans maillage constitue un outil numérique très intéressant pour la modélisation de certains problèmes complexes comme la fracturation de solides. Cette technique, développée au départ pour simuler le comportement de gaz a été par la suite étendue aux fluides puis aux solides mais dans ce dernier cas d'importants problèmes de stabilité apparaissent. Les origines de ces instabilités ont été identifiées par la communauté SPH et des solutions ont été proposées. Une description de ces différentes solutions est présentée ici. Parmi elles le recours à une formulation SPH lagrangienne totale semble le plus efficace pour stabiliser la méthode. Dans le même temps cette formulation peut être couplée à la technique des stress points qui permet en particulier d'améliorer la précision et la vitesse de convergence de la méthode au prix cependant d'une augmentation du coût de calcul.

KEYWORDS: SPH, stability, total Lagrangian formulation.

MOTS-CLÉS : SPH, stabilité, formulation lagrangienne totale.

1. Introduction

Meshfree methods are now very appealing numerical tools for modelling severe distortions, failure and fragmentations of solids, with many advantages as compared to the classical finite element methods. The Smoothed Particle Hydrodynamics method (SPH) was the first meshfree method to be proposed (Monaghan *et al.*, 1977) and was first utilized for gas dynamic problems. This method was later extended to fluid and solid modelling but difficulties were also identified such as important instability problems. The purpose of this paper is to give an overview of these problems and of the numerical solutions developed by the SPH community to solve them.

2. The SPH method

2.1. Principle of the method

As mentioned above the SPH method can be considered as a meshless particle method. The interactions between the particles are determined by interpolation from information at the SPH particles using an interpolation function called kernel function.

The basis of the method comes from the well known result for a function:

$$f(\vec{x}) = \int_{\Omega} f(\vec{y}) \delta(\vec{x} - \vec{y}) d\Omega \quad [1]$$

Where δ is a Dirac distribution and \vec{x} \vec{y} are position vectors.

This expression can be approximated by replacing the Dirac function by a kernel function $W(\vec{x}, h)$ where h determines the size of the support domain (the part of the domain where W is nonzero) and is characterized by:

$$\lim_{h \rightarrow 0} W(\vec{x} - \vec{y}, h) = \delta(\vec{x} - \vec{y})$$

The kernel widely used in SPH is a cubic spline kernel called B-spline which has the form:

$$W(r, h) = C \begin{cases} \frac{3}{2} \left[\frac{2}{3} - \left(\frac{r}{h} \right)^2 + \frac{1}{2} \left(\frac{r}{h} \right)^3 \right] & 0 \leq \frac{r}{h} \leq 1 \\ \frac{1}{4} \left(2 - \frac{r}{h} \right)^3 & 1 \leq \frac{r}{h} \leq 2 \\ 0 & r > 2h \end{cases} \quad \text{where } r = d(\vec{x}, \vec{y})$$

The parameter C is determined in order to ensure the normality property:

$$\int_{\Omega} W(\vec{x} - \vec{y}, h) d\Omega = 1$$

It implies that for 1D, 2D and 3D problems the values of C are respectively $2/3h$, $10/7\pi h^2$, $1/\pi h^3$. For the 3D case the kernel is shown in Figure 1.

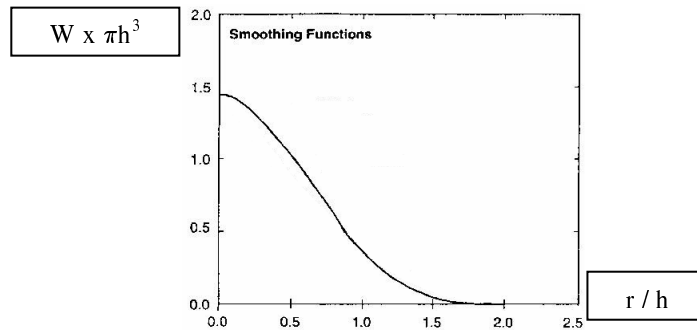


Figure 1. 3D Kernel function

Then Equation [1] becomes:

$$f(\vec{x}) \approx \langle f(\vec{x}) \rangle = \int_{\Omega} f(\vec{y}) \cdot W(\vec{x} - \vec{y}, h) d\Omega \tag{2}$$

Using integration by parts and the fact that the integrals on the boundary vanish at infinity an approximation of the gradient of a function can be obtained:

$$\nabla f(\vec{x}) \approx \langle \nabla f(\vec{x}) \rangle = \int_{\Omega} f(\vec{y}) \cdot \nabla W(\vec{x} - \vec{y}, h) d\Omega \tag{3}$$

These two last equations can be put in a discrete form at each SPH particle (denoted i) by replacing the integrals by summation over its neighbouring particles (denoted j):

$$\langle f \rangle_i = \sum_j f_j \cdot W(\vec{x}_i - \vec{x}_j, h) V_j \quad V_j = \frac{m_j}{\rho_j} \tag{4}$$

In Equation [4] m_j is the mass associated to each particle (constant in time) and ρ_j is the density. In the same way the following expression can be established:

$$\langle \nabla f \rangle_i = \sum_j \frac{m_j}{\rho_j} f_j \cdot \nabla W(\bar{x}_i - \bar{x}_j, h) \quad [5]$$

NOTE. — Later for simplicity $W(\bar{x}_i - \bar{x}_j, h)$ will be noted W_{ij} .

The concept of neighbourhood for a particle introduced here is in fact constituted by all the particles for which W_{ij} is nonzero which means in fact that the distance between i and j is less than $2h$ as shown in Figure 1.

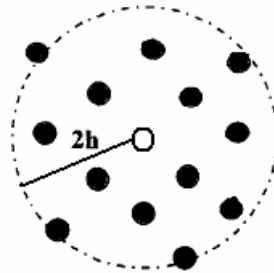


Figure 2. SPH particle neighbourhood

2.2. Lack of consistency

One of the major drawbacks of the SPH method is its lack of consistency. Consistency is the ability of an interpolation or an approximation to reproduce an imposed field. Often, consistency is obtained if polynomial can be represented exactly. In order to achieve good accuracy and convergence zero order and first order consistency requirements must be met by the SPH approximations [4], [5]. It can be shown that the first order consistency condition is not respected which means that for a constant function $f(\bar{x}) = 1$:

$$\langle \nabla f \rangle_i = \sum_j \frac{m_j}{\rho_j} \cdot W_{ij} \neq 0$$

The same problem appears with the first order consistency for $f(\bar{x}) = x$:

$$\left\langle \frac{\partial f}{\partial x} \right\rangle_i = \sum_j \frac{m_j}{\rho_j} x_j \cdot W_{ij} \neq 1$$

To enforce these two fundamental properties some modifications of the expression [5] must be made. A differential form of [5] is introduced to ensure the nullity of the gradient of a constant field:

$$\langle \nabla f \rangle_i = \sum_j \frac{m_j}{\rho_j} (f(x_j) - f(x_i)) W_{ij} \quad [6]$$

This last expression was then normalised (Johnson and Beissel,) and (Randles & Libersky, 1996) in order to achieve both zero and first order consistencies. The normalisation takes the form of a correcting matrix B:

$$\left(\frac{\partial f}{\partial x^\beta} \right)_i = \left[\sum_j m_j \frac{f_j - f_i}{\rho_j} \frac{\partial W_{ij}}{\partial x_i^\beta} \right] B^{i\beta} \quad [7]$$

The correcting matrix is obtained by inverting a matrix H defined by:

$$H^{i\beta} = \sum_j m_j \frac{x_j^\beta - x_i^\beta}{\rho_j} \frac{dW_{ij}}{dx_i^\beta}$$

NOTE. — The subscript B will be omitted in the following equations of the paper in order to simplify the presentation.

The consistency is a fundamental property for a meshless method. It was the starting point of the development of several other meshfree methods such as MLSPH and RKPM, where more sophisticated techniques are used in order to ensure higher order of consistency.

2.3. SPH equations for a continuum

As seen above the SPH formulation [7] allows determining an approximation of the gradient or the divergent of a field. The conservation laws of continuum dynamics can then be applied to each particle. The first of these is the continuity equation:

$$\frac{d\rho}{dt} + \rho \times \text{div}(\vec{v}) = 0$$

Using the SPH framework it becomes:

$$\frac{d\rho_i}{dt} = \rho_i \sum_j m_j \frac{1}{\rho_j} (\vec{v}_i - \vec{v}_j) \cdot \vec{\nabla}_i W_{ij} \quad [8]$$

The second equation is the conservation of momentum:

$$\rho \frac{d\vec{v}}{dt} = \text{div}(\underline{\underline{\sigma}})$$

This becomes:

$$\rho_i \frac{d\vec{v}_i}{dt} = \sum_j m^j \frac{1}{\rho_j} (\underline{\underline{\sigma}}_i - \underline{\underline{\sigma}}_j) \cdot \vec{\nabla}_i \cdot W_{ij} \quad [9]$$

The following equation is also widely used in SPH because of its symmetry:

$$\frac{d\vec{v}_i}{dt} = - \sum_j m^j \left(\frac{\underline{\underline{\sigma}}_i}{\rho_i^2} + \frac{\underline{\underline{\sigma}}_j}{\rho_j^2} + \Pi_{ij} \right) \vec{\nabla}_i \cdot W_{ij} \quad [10]$$

NOTE. — In Equations [10] Π_{ij} is an artificial viscosity used in order to stabilise the numerical scheme.

NOTE. — It can be seen that using the Equation [9] the contribution of a neighbouring particle j to the acceleration of a particle i is the same as the one of j to the acceleration of i, which means in fact that the force exerted by the particle i on j is the same as the one exerted by j on i.

This formalism can be applied for a wide variety of materials including gas, fluids and solids. In the case of solid material the Cauchy stress tensors used in [9], [10] come from strain tensors ε obtained using the same framework:

$$\varepsilon_{\alpha\beta}(i) = \frac{1}{2} \sum_j \frac{m^j}{\rho_i} \left[(u_\alpha(i) - u_\alpha(j)) \frac{\partial W_{ij}}{\partial x_{i\beta}} + (u_\beta(i) - u_\beta(j)) \frac{\partial W_{ij}}{\partial x_{i\alpha}} \right] \quad [11]$$

3. Stability problems

3.1. Tensile instability

The SPH method applied to solid materials suffers from instability problems. They become obvious in some very simple cases such as deformation of elastic square section beam (made of steel $E=2e11$ Pa, $\nu=0.3$ and $\rho=7800$ kg/m³) submitted to a traction load increasing linearly with time. The evolution of the longitudinal displacement at the end of the beam is plotted on Figure 3. It is very far from the analytical solution which is linear. For example at the end of the calculation ($t = 2500 \mu\text{s}$) the displacement is hundred times bigger than the analytical value. In fact the response of the bar is correct only at the beginning of the computation for very small deformations. Then numerical fractures occur as can be seen on Figure 4.

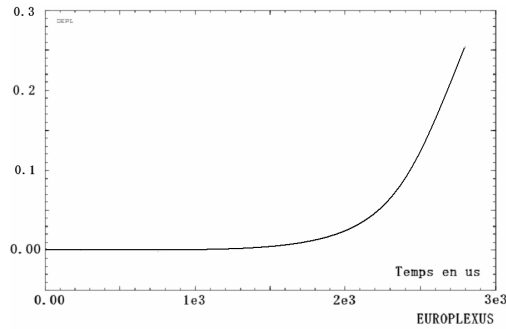


Figure 3. Evolution of the displacement at the end of the beam

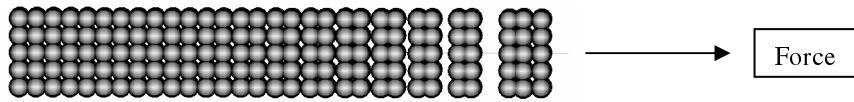


Figure 4. Numerical fractures observed on the beam submitted to traction load

This makes the standard SPH method unable to represent accurately the behaviour of a solid body unless the deformations are very small. Another kind of instabilities can be observed for the same beam submitted to initial traction stress or compression stress by applying a small perturbation on a single particle. Here we perturb the initial velocity field of the beam. The evolution of the velocity of the perturbed particle is plotted on Figure 5.

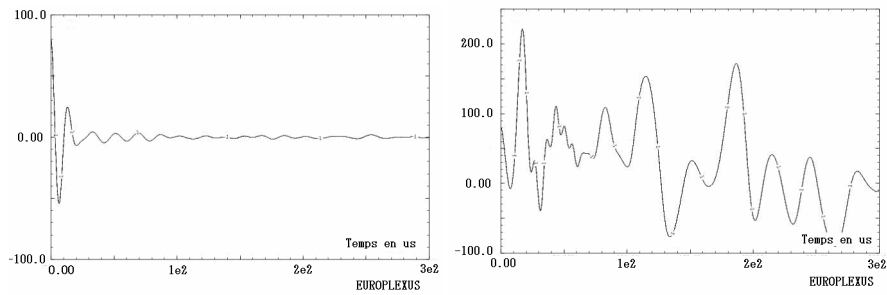


Figure 5. Evolution of the velocity of the perturbed particle for initial compression stress (left) and traction stress (right)

This example is very close to the one that can be found in (Belyschko *et al.*, 2000) and which illustrates the instability of the standard SPH method. In the

traction case the perturbation grows more significantly showing that the method is unstable even for small deformations.

These phenomena were first studied by Swegle and co-workers (Swegle *et al.*, 1995) by a Von-Neuman stability analysis on a 1D SPH formulation. They related SPH instability problems to traction state coupled to the sign of the second derivative of the kernel function. This is the origin of the name Tensile Instability widely used in the SPH literature and the starting point of many developments achieved by the SPH community. A good overview of this work can be found in (Belytschko *et al.*, 2000). This paper gives also a very complete analysis of what causes the instabilities. Three kinds of instabilities coming from different sources are then identified:

- instability of the continuum equations;
- the tensile instability;
- the reduced integration.

By achieving a Von Neuman stability analysis of the continuum equations Belytschko *et al.*, revealed instability in the case of strain softening (material modulus sufficiently negative) or under high compressive loads. The same analysis of the discrete equations obtained within the SPH framework has been achieved and revealed the tensile instability previously identified by Swegle *et al.*, This can be of course related to the results shown on the Figure 5.

The third kind of instability comes from the reduced integration. It is due to the fact that all SPH variables for a given particle are located in a single point. This instability is similar to the well-known problem of hourglass in finite element literature. Under integration can be easily understood by studying the 1D finite difference method which is in fact very similar to the 1D SPH method. The first derivative of a field U for a particle i with neighbours $i+1$ and $i-1$ and a uniform distance h between particles is then:

$$\left(\frac{dU}{dx}\right)_i = \frac{U_{i+1} - U_{i-1}}{2h} \quad [12]$$

The second derivative of U is:

$$\left(\frac{d^2U}{dx^2}\right)_i = \frac{(dU/dx)_{i+1} - (dU/dx)_{i-1}}{2h} \quad [13]$$

Using [12] the Equation [13] becomes:

$$\left(\frac{d^2U}{dx^2}\right)_i = \frac{U_{i+2} + U_{i-2} - 2U_i}{4h^2}$$

This expression of the second derivative is the same as the one which should be obtained with a two times coarser discretization. For a one dimensional formulation the acceleration of a particle at each time step is computed by:

$$a_i = \frac{1}{\rho_i} \left(\frac{d\sigma}{dx} \right)_i = \frac{E}{\rho_i} \left(\frac{d\varepsilon}{dx} \right)_i = \frac{E}{\rho_i} \left(\frac{d^2U}{dx^2} \right)_i \quad [14]$$

This becomes:

$$a_i = \frac{E}{\rho_i} \frac{U_{i+2} + U_{i-2} - 2U_i}{4h^2}$$

It is important to notice that the acceleration of a particle is, in this case, totally independent from the displacements of its two closest neighbours $i+1$ and $i-1$. It means that the model is in fact constituted by two independent sets of particles $i-2, i, i+2$ and $i-3, i-1, i+1, i+3$. If the loads and the boundary conditions applied to these two sets of particles are the same then the displacements of two following particles belonging to different sets will also be the same. It means that in this case during the computation the particles will stay stick together and the displacement field will be defined by $U_i = U_{i+1}$ or $U_i = U_{i-1}$.

Of course the situation is more complex for a 1D SPH code because of the nonuniform particle spacing and the SPH framework which takes into account more neighbouring particles for the evaluation of the gradient. The two sets of particles are then not totally independent, but the behaviour of the particles is however quite similar. Even in a three dimensional case this manifestation of the underintegration can be observed as can be seen on Figure 4 where layers of particles stay stick together.

This clustering of particles leads the grid of particles becoming less regular which affect the quality of the computation of the accelerations used to update the position of the particles. This makes the distortions growing and leading to numerical fractures because of excessive distance between two particles belonging to different clusters.

Using the Belytshcko's analysis it is also possible to explain why the instabilities occur mainly for solid materials and not for fluid or gas. Of course for a fluid or a gas there can't be any traction state except in some cases including cavitations where the tensile stress stays very low. This is the reason why it's very difficult for the tensile instability to appear. In the same way fluid or gas SPH formulations are less sensitive to underintegration because the stress tensor is constituted mainly by hydrostatic pressure which is computed from the density by a pressure law. The acceleration is then not related to the second derivative of the displacement field.

3.2. Conservative smoothing

As mentioned previously the stability problems have been widely identified and documented but solutions were also proposed by researchers. The first was from Swegle, Wen and Hicks (Swegle *et al.*, 1994) with the introduction of the conservative smoothing in the 1D SPH method. The purpose of this technique was to remove spurious short wavelength oscillations (wavelength less than distance between particles) and in particular those from underintegration by applying a filter to the velocities. The velocity of each particle U_i is replaced by a new one computed from:

$$\hat{U}_i = U_i + \alpha[0.5(U_{i-1} + U_{i+1}) - U_i] \quad [15]$$

NOTE. — α is a parameter such as $0 < \alpha < 0.5$; $i-1$ and $i+1$ correspond to the closest neighbours of the particle i .

The effect on the hourglass phenomenon of the filtering described above can be understood easily. As mentioned previously because of the underintegration displacement and velocity fields can be severely distorted. For example in the case of a supposed linear velocity field the values computed with the SPH approximation ($U_i = U_{i+1}$) before and after the filtering are shown on Figure 6. The distortions caused by the underintegration are clearly removed:

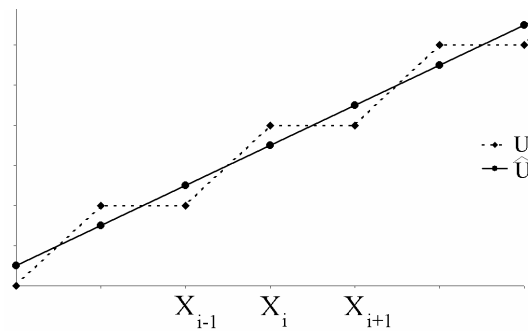


Figure 6. Effect of the 1D conservative smoothing with $\alpha=0.5$

This filtering was extended to three dimensional cases in (Randles & Libersky, 1996):

$$\hat{U}_i^\beta = U_i^\beta + \alpha \left[\frac{\sum_j (m_j U_i^\beta W_{ij} / \rho_j)}{\sum_j (m_j W_{ij} / \rho_j)} - U_i^\beta \right] \quad [16]$$

This technique is very attractive because of its simplicity and its low computational cost. It seems also to be very effective for 1D problem and in some simple 3D cases. For example the elastic bar submitted to traction can now undergo moderate deformation without numerical fractures and the response shown on Figure 7 stays very close to the analytical solution. Illustrations of the removal of the instabilities in problems involving transient stress fields can be found in the papers of Sweigle and Randles & Libersky.

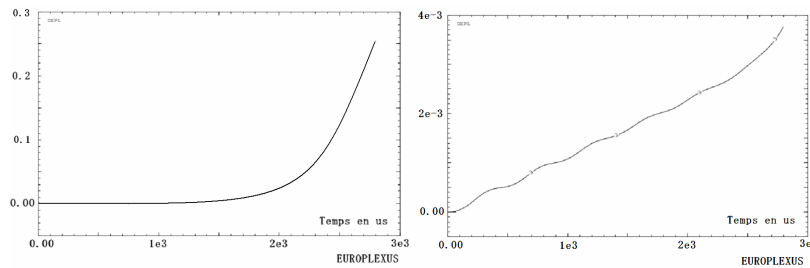


Figure 7. Elongation at the end of a beam without (left) and with (right) filtering

NOTE. — On the right graph the vertical scale is ten times smaller than on the left one.

But for geometrically more complex calculations the dissipation introduced by the method seems too excessive. The response of the previous beam in free bending oscillations exhibits excessive damping, see Figure 8. The same kind of problem occurs with elasto-plastic materials where plastic deformations are artificially reduced.

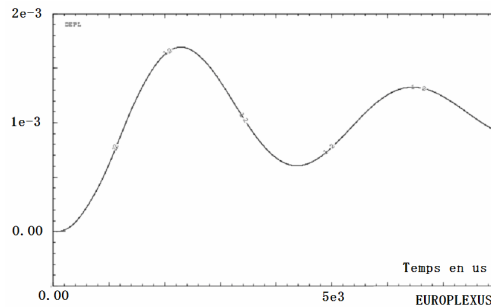


Figure 8. Evolution of the deflection at the end of a beam in free bending oscillations

As previously mentioned, the filtering eliminates the oscillations whose wavelength is less or equal than the distance between particles. It means that the discretization must be fine enough in order to ensure that the physical response of the structure is not affected by the filtering. The particle spacing must also stay quite uniform to avoid excessive dissipation.

This makes difficult the use of the conservative smoothing method. It explains the reason why the development of other techniques for stabilizing SPH and other meshless methods had been pursued.

3.3. Artificial stress

A different approach was proposed by Monaghan, Swift and Gray (Monaghan *et al.*, 2001). The purpose here is to stabilise the SPH equations by applying artificial forces onto the particles. The Equation [10] becomes:

$$\frac{d\bar{v}_i}{dt} = -\sum_j m^j \left(\frac{\sigma_i}{\rho_i^2} + \frac{\sigma_j}{\rho_j^2} + \Pi_{ij} - f_{ij}^n \left(\frac{R_i}{\rho_i^2} + \frac{R_j}{\rho_j^2} \right) \right) \bar{\nabla}_i \cdot W_{ij} \quad [17]$$

These stabilising terms are determined in order to satisfy a stability criterion provided by a stability analysis. The tensor R is called artificial stress. It is computed in the coordinate system where the stress tensor is diagonal. Its values are nonzero only in the case of tensile stress:

$$\text{If } \sigma_i^{aa} > 0 \text{ then } R_i^{aa} = -\eta \sigma_i^{aa} \text{ with } 0.3 \leq \eta \leq 0.8$$

$$\text{If } \sigma_i^{aa} < 0 \text{ then } R_i^{aa} = 0$$

Then R is rotated to the global coordinate system. The value of f_{ij} in [17] is defined by:

$$(f_{ij})^n = \left(\frac{W_{ij}}{W(r=h, h)} \right)^n \text{ with } n=3 \text{ or } n=4$$

As mentioned in (Monaghan *et al.*, 2001) this method seems to be very effective to remove numerical fractures but it suffers from the same drawback as the conservative smoothing. It works properly only if the discretization is fine enough. This can be explained by the fact that the artificial forces added by the method act only on a very small scale (which size is the interparticle distance). But if the mesh is too coarse they interfere with the global response of the structure and affect the precision of the method. Moreover the parameter η appears to have a great influence

on the numerical results and the best value of η can be different for different test cases.

3.4. Stress points

The underintegration problem described above led some researchers (Dyka *et al.*, 1997) to suggest adding to the classical SPH framework a new set of pseudo-particles called stress points. They carry stress whereas classical SPH particles carry velocity and position. Using again, as was done by Dyka, the comparison with the 1D finite difference method it can be shown that the hourglass phenomenon is clearly removed. For a 1D uniform particle spacing the stress $\sigma_{i+1/2}$ computed on the stress point $i+1/2$ inserted between SPH particles i and $i+1$ is defined by:



$$\sigma_{i+1/2} = E \frac{dU}{dx} = E \frac{U_{i+1} - U_i}{h} \tag{18}$$

Using [18] Equation [14] becomes:

$$a_i = \frac{1}{\rho_i} \left(\frac{d\sigma}{dx} \right)_i = \frac{1}{\rho_i} \frac{\sigma_{i+1/2} - \sigma_{i-1/2}}{h} = \frac{E}{\rho_i} \frac{U_{i+1} + U_{i-1} - 2U_i}{h^2}$$

The second derivative of the displacement field U is then correctly computed. This strategy was extended to 2D situation in (Randles & Libersky, 2000). A simple example of the initial mapping of the stress points in a SPH discretization is shown on Figure 9. More sophisticated solutions to place stress points on nonuniform particle spacing have been employed, such as for example Voronoi diagrams. Once placed, the stress points need also to be moved as the SPH particles do. For this purpose stress points velocities are interpolated from the ones of the surrounding SPH particles.

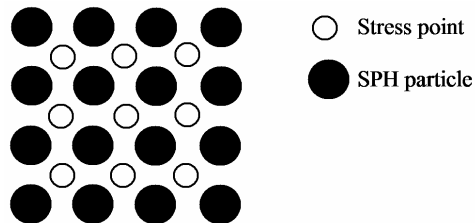


Figure 9. A simple way to place stress points in 2D case

As shown by Dyka the use of the stress points can improve significantly the stability of the SPH method. But further analysis (Belytscko *et al.*, 2000) revealed that it removes only the underintegration and is unable to eliminate the tensile instability. In the same time it can be shown (Belytschko *et al.*, 2004) that this technique can improve significantly the precision and the convergence rate of the method.

4. Total lagrangian SPH formulation

4.1. Total lagrangian formulation

The tensile instability is related to the use of an eulerian kernel usually used in the SPH framework [6]. In (Belytscko *et al.*, 2000) another very interesting idea to solve instability problems has been introduced. According to (Belytscko *et al.*, 2000) it can be shown that the use of a new type of kernel called lagrangian kernel can remove the tensile instability. The lagrangian kernel W_0 is the same as the eulerian one W but it is defined on the initial configuration. It means that:

$$W_{ij}^0 = W(\vec{x}_i^0 - \vec{x}_j^0, h_0)$$

where \vec{x}_i^0 and \vec{x}_j^0 are the initial position vectors of the particle i and j .

Using this Lagrangian kernel means that the initial configuration is now the reference configuration and it implies that the formulation becomes a total Lagrangian formulation. In the Equation [10] the Cauchy stress tensor is then replaced by the transpose of the first Piola-Kirchhoff stress tensor P and [10] becomes:

$$\frac{d\vec{v}_i}{dt} = -\sum_j m^j \left(\frac{P_i}{\rho_{0i}^2} + \frac{P_j}{\rho_{0j}^2} + \Pi_{ij} \right) \vec{\nabla}_{0i} \cdot W_{0ij} \quad [19]$$

The first Piola-Kirchhoff stress tensor is obtained from the Green-Lagrange strain tensor computed by:

$$E_{\alpha\beta}(i) = \frac{1}{2} \sum_j \frac{m^j}{\rho_{0i}} \left[(u_\alpha(i) - u_\alpha(j)) \frac{\partial W_{0ij}}{\partial x_{i\beta}^0} + (u_\beta(i) - u_\beta(j)) \frac{\partial W_{0ij}}{\partial x_{i\alpha}^0} \right]$$

The gradient matrix F is determined by the similar formula:

$$F_{\alpha\beta}(i) = \frac{1}{2} \sum_j \frac{m^j}{\rho_{0i}} \left[(x_\alpha(i) - x_\alpha(j)) \frac{\partial W_{0ij}}{\partial x_{i\beta}^0} + (x_\beta(i) - x_\beta(j)) \frac{\partial W_{0ij}}{\partial x_{i\alpha}^0} \right]$$

A very interesting feature of this new SPH formulation is that we don't need to update some quantities attached to particles. As can be seen in formula [19] the current density is no longer used which makes the continuity equation and the updating of the density at each time step useless. In the same way as previously described the initial configuration is now the reference configuration and the interpolations such as mentioned in [7] are now computed using a Lagrangian kernel on the initial neighbourhood of each SPH particle. The neighbourhood search which is a very expensive operation in terms of computational costs is now achieved on each particle only once at the first time step. This makes the total Lagrangian (TL) SPH formulation less CPU consuming than the classical updated Lagrangian formulation.

4.2. Stability improvements

In order to illustrate the robustness of the total Lagrangian formulation the bending of the previously mentioned square section beam is simulated with the classic SPH method and the TL method. As can be seen on Figure 10, with this new formulation the beam can undergo large deflections and relatively large deformations without suffering from the numerical fractures that occur with the classical SPH method.

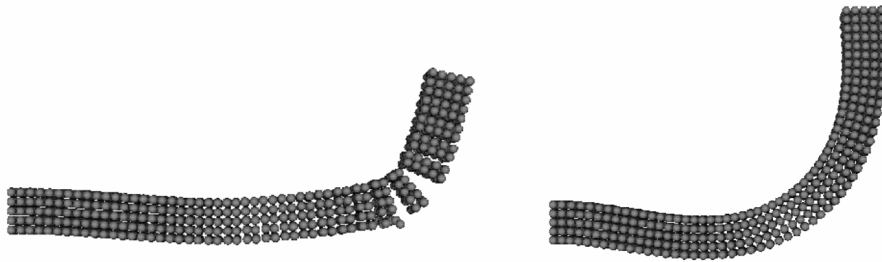


Figure 10. *Bending of a beam with classical SPH (left) and total lagrangian (right)*

The results shown on Figure 5 can be compared to the ones obtained with the total Lagrangian method plotted on Figure 11. The perturbation disappears after several oscillations.

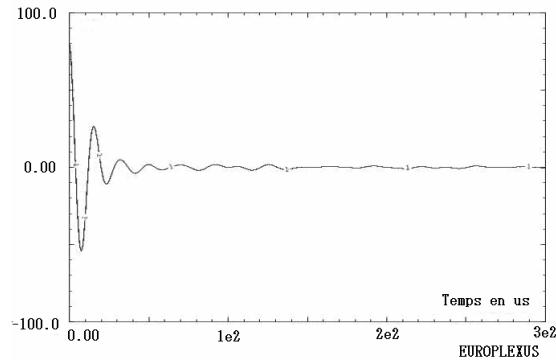


Figure 11. Evolution of the velocity of the perturbed particle with initial traction stress (3 Gpa) (see Figure 5)

The robustness of the method is clearly improved. The stabilisation works well even for relatively coarse discretization with no distortion on the structural response and no dissipation. In the same way this stabilizing solution does not require to set parameters compared to the previous ones.

In fact the tensile instability is removed and the underintegration problem seems also to be alleviated. The reference configuration is the initial which remains regular and undeformed along the calculation. The SPH equations are thus not affected by the distortion of the displacement field due to the hourglass phenomenon and the resulting instabilities can't grow. But according to (Belytchko *et al.*, 2000) the underintegration is however not totally removed and can still reduce the precision and the convergence rate of the method as for the classical SPH formulation. That's why the best way to achieve both stability and precision seems to be the coupling of both the total Lagrangian formulation and the Stress points approach as was done in (Belytscko *et al.*, 2004) despite an increase in computational cost. The stress points method is also much easier to use with the total Lagrangian formulation because the pseudo-particles are placed in the initial configuration and then don't need to be moved.

4.3. Fractures and contact in SPH TL formulation

As mentioned above using the SPH total Lagrangian formulation the neighbourhood of the particles are not updated. This makes the method not suitable for the modelling of gas or fluids (or solids with very large deformations) where the particle spacing can be severely distorted. But in the case of solids undergoing moderate deformations before failure each particle keeps the same neighbours during the calculation. The particles' neighbourhood is modified only if fractures or

contacts happen. Fractures can be easily handled by the method using a rupture criterion. If fractures occur then interactions between some particles are removed, which means that they are pulled out from the initial neighbourhood of their neighbours. Some more accurate techniques can be implemented to deal with fractures or crack growth such as the one proposed in (Rabzuck & Belytschko, 2004) which is a local enrichment of the formulation like the XFEM method for finite element method.

The problem of contact within the total Lagrangian formulation can also be alleviated by using an impact/contact algorithm such as the pinball method (Belytschko *et al.*, 1991). It means that in order to detect contact a specific neighbourhood search is performed at each time step only for the boundary particles of the two contacting bodies. If interpenetration is detected the Contact forces are computed by the use of lagrangian multipliers and applied on the concerned particles as external forces.

5. Conclusion

This paper has presented a review of the existing numerical techniques based on the SPH formulation and used to deal with solid mechanics applications. The usual SPH method based on the updated Lagrangian formulation exhibit artificial numerical fractures and instabilities. It is shown that one of the best choices to avoid unstable calculations is to use the total Lagrangian formulation which is stable and also computationally efficient because any update of the neighbours is necessary, unless contact or fracture take place. The case of fracture can be rather simply simulated by breaking the links between particles. The combination of this method with a usual SPH method to solve fluid-structure interaction problems shall be presented in a near future.

Acknowledgements

The authors wish to express their thanks to EDF R&D for its financial support.

6. References

- Belytschko T., Neal M.O., "Contact-Impact by the Pinball method with penalty and Lagrangian Methods", *International journal for numerical methods in engineering*, Vol. 31, 1991, p. 547-572.
- Belytschko T., Guo Y., Liu W.K., Xiao S.P., "A unified stability analysis of meshless particle methods", *International journal for numerical methods in engineering*, Vol. 40, 2000, p. 1359-1400.

- Belytschko T., Rabczuk T., Xiao S.P., “Stable particle methods based on Lagrangian kernels”, *Computer methods in applied mechanics and engineering*, Vol. 193, 2004, p. 1035-1063.
- Dyka, Randles P.W., Ingel R.P., “Stress points for tension instability”, *International journal for numerical methods in engineering*, Vol. 40, 1997, p. 2325-2341.
- Gingold R.A., Monaghan J.J., “Smoothed particle hydrodynamics: theory and application to non-spherical stars”, *Mon. Not. R. astr. Soc.*, Vol. 181, 1977, p. 375.
- Gray J.P., Monaghan J.J., “SPH elastic dynamics”, *Computer methods in applied mechanics and engineering*, Vol. 190, 2001, p. 6641-6662.
- Johnson G.R., Stryck R.A., Beissel S.R., “SPH for high velocity impact”, *Computer methods in applied mechanics and engineering*, Vol. 139, 1996, p. 347-373.
- Rabczuk T., Belytschko T., “Cracking particles: a simplified meshfree method for arbitrary evolving cracks”, *International journal for numerical methods in engineering*, Vol. 61, 2004, p. 2316-2343.
- Randles P.W., Libersky L.D., “Smoothed Particle Hydrodynamics: Some recent improvements and applications”, *Computer methods in applied mechanics and engineering*, Vol. 139, 1996, p. 375-408.
- Randles P.W., Libersky L.D., “Normalized SPH with stress points”, *International journal for numerical methods in engineering*, Vol. 48, 2000, p. 1445-1462.
- Swegle J.W., Hicks D.L., Wen Y., Stabilizing SPH with conservative smoothing, Sandia Report, SAND94-1932, 1994.